Appendix O

Detection of Tidal Turbine Noise: A Pre-Installation Case Study for Admiralty Inlet, Puget Sound

Detection of tidal turbine noise: A pre-installation case study for Admiralty Inlet, Puget Sound, Washington (USA)

B. Polagye, C. Bassett; Northwest National Marine Renewable Energy Center, University of Washington, Seattle, Washington, United States

Jason Wood; Sea Mammal Research Unit, Ltd., Friday Harbor, Washington, United States

S. Barr; OpenHydro, Ltd., Greenore, Ireland

Abstract

The development of sustainable tidal power generation schemes is contingent upon demonstrating the environmental compatibility of this technology. Among the environmental uncertainties is the effect that the noise generated by tidal turbines might have on fish and marine mammals. Consequently, it is desirable to better understand these interactions through pilot-scale monitoring before commercial-scale deployments are undertaken. Effective monitoring plans must account for the extent of noise and the potential for this noise to cause detectable changes. This study presents a case study for a proposed pilot project that synthesizes available measurements of turbine noise and underwater ambient noise to evaluate the effectiveness of studies to characterize turbine noise and the marine mammal response to this noise. Because both turbine noise and ambient noise vary in time, the description is probabilistic. The time distribution of turbine noise is derived from measurements of a similar tidal turbine and convolved with the time distribution of ambient noise in the proposed project area. Results suggest that characterizing turbine noise and studying marine mammal responsiveness at this location will be challenging due to existing ambient noise associated with high vessel traffic density and sediment transport. The case study provides instructive guidance for high-priority data needs and an analysis framework for evaluating acoustic effects of tidal energy projects.

1 Introduction

Sustainable power generation schemes must be technically, economically, socially, and environmentally viable. Consequently, a renewable resource is a necessary, but not sufficient, condition for sustainable power generation. As new power generation schemes are developed, it is desirable to evaluate their sustainability at the pilot scale. This enables early results to inform the engineering design process and improve sustainability.

Hydrokinetic power generation harnesses the kinetic power in swiftly moving tidal currents. Tidal hydrokinetic power is predictable, intense, and often in close proximity to electrical loads. It may also be more environmentally compatible than tidal barrage power generation, which relies on impoundment similar to conventional hydropower (Twidell and Weir, 2006). Environmental impacts are possible from large-scale, hydrokinetic tidal power generation, but uncertain (Cada et al., 2007; Polagye et al., 2011a) in that the severity and frequency of possible stressor-receptor interactions has not been established. Among the areas of concern are acoustic impacts, whereby the noise from tidal turbine operation could lead to physiological (e.g., temporary threshold shift) or behavioral alteration for fish, diving birds, or marine mammals. Similar concerns exist for other forms of anthropogenic noise, such as vessel traffic (Hatch et al., 2008; McQuinn et al., 2011; McKenna et al., 2012; Bassett et al., submitted) and are

grouped under the broader heading of Population Consequences of Acoustic Disturbances (PCAD) (NRC, 2005).

Given the broad range of potential environmental impacts and limited resources available (both private and public), prioritization of environmental studies at pilot projects is required (Polagye et al., 2011a). Pre-installation estimates for the acoustic effects of a tidal energy project are, therefore, needed to structure study plans that will likely provide useful information about the extent of the acoustic stressor and receptor (e.g., marine mammal) response. Such estimates are site-specific and must include contextual information about pre-installation ambient noise. Since ambient noise and tidal turbine noise vary in time, any estimate is probabilistic in nature.

This paper presents a case study for a pre-installation estimate of the acoustic effects of a pilot tidal power project proposed in northern Admiralty Inlet, Puget Sound, Washington (USA). The objective is to highlight knowledge gaps and suggest a methodology for assessing the environmental consequences of turbine noise in a probabilistic manner. This type of problem (attempting to develop post-installation study plans with incomplete data) will be commonly encountered during tidal energy project development for the foreseeable future.

The probability of detecting turbine noise relative to other sources of ambient noise may be expressed in terms of the "signal excess" (NRC, 2003)

$$SE = RL - NL \tag{1}$$

where *SE* is the signal excess, *RL* is the received level of the noise source, and *NL* is the background ambient noise. If the signal excess is positive, the noise will be detected by the receiver. The received level is related to the source level (*SL*) by

$$RL = SL - TL + AG \tag{2}$$

where *TL* is the transmission loss and *AG* is the gain associated with signal processing (either biological or computational). Therefore, in order to evaluate the detection of turbine noise, information is required about the noise generated by the turbine and ambient noise. These quantities are frequency-dependent and could be interpreted in spectral, one-third octave, octave, and decadal levels, M-weighted broadband levels (Southhall et al. 2007), or unweighted broadband levels. For the purposes of this case study, detection statistics are presented in one-third octave bands (TOBs) since this is common practice in describing noise exposure in marine mammals as it approximates the way noise is integrated by the auditory system of marine mammals (Madsen et al., 2006; Miller, 2006; Richardson et al., 1995). One-third octave band center frequencies are 100, 125, 160, 200, 250, 315, 400, 500, 630, and 800 Hz (repeating by a power of ten for lower and higher frequency decade).

Section 2 provides background and methodology for the case study. Background information includes existing noise measurements from the type of turbine proposed for deployment and site-specific ambient noise in the pilot project area. The study methodology consists of a model to estimate received noise levels in the vicinity of the proposed pilot project and probabilistic detection and/or responsiveness by a receiver (e.g., hydrophone, fish, marine mammal). In both cases, the methodology emphasizes simplicity and transparency (e.g., use of the SONAR equation to estimate received levels of turbine noise rather than a parabolic equation model). Section 3 presents case study results for detection of turbine noise for different types of receivers in the context of ambient noise variability.

Section 4 discusses the implications of these results towards the design of environmental study plans for the proposed pilot project and the distance at which acoustic cues might be detected by fish and marine mammals. Section 4.2 concludes with a summary of results and recommendations for future work to close knowledge gaps.

2 Background and Methodology

2.1 Project Description

Snohomish Public Utility District (www.snopud.com) and OpenHydro, Ltd. (www.openhydro.com) have proposed a pilot-scale tidal energy project in northern Admiralty Inlet, Puget Sound, Washington. Water depth in the project area varies between 50 and 60 m and tidal currents at this location exceed 3 m/s. Numerous species of fish and marine mammals are known to occur in the project area (Snohomish PUD, 2009). The project consists of two turbines located 70 m apart on the seabed. The turbines have shrouded, horizontal axis rotors, are deployed on gravity-anchored foundations (Figure 1), and are connected to shore by submarine power cables. This type of turbine has a single moving part – the multi-bladed rotor is supported by water-lubricated rim bearings. Power take-off is by a direct-drive permanent magnet generator in the shroud. The turbine blades are symmetric, fixed pitch and operate at a constant tip-speed ratio. Project parameters are summarized in Table 1. As for most pilot projects, operating parameters are subject to change as the technology evolves. The size of these turbines and the overall scale of the project are pre-commercial, in that the primary objective of the project is to deliver engineering, environmental, and economic data, rather than cost-competitive, utility-scale power generation. These data are essential to establish the feasibility of larger-scale power generation projects.

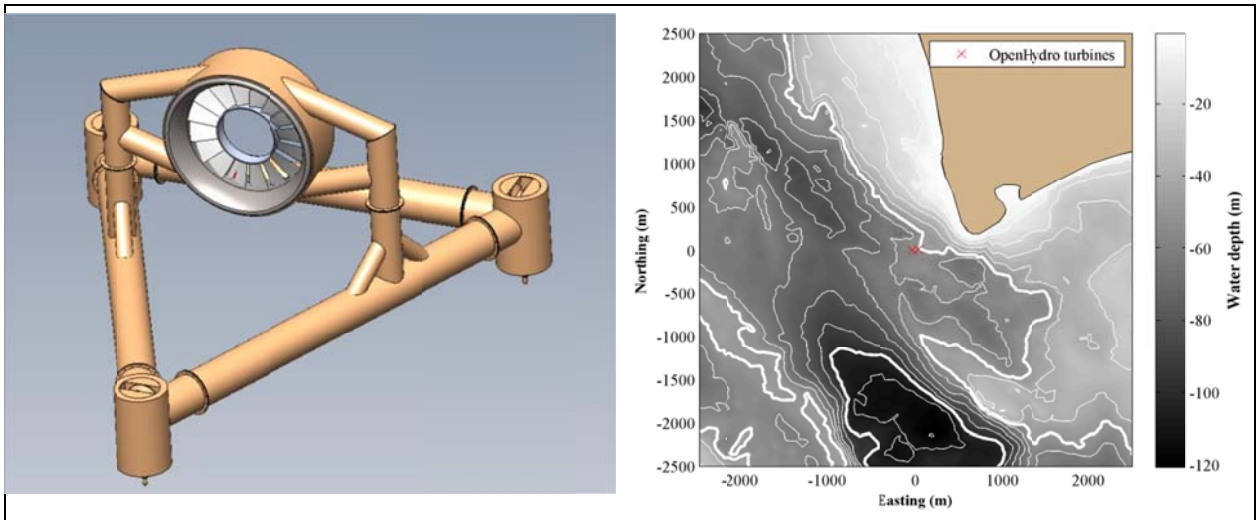

(a) 6 m diameter OpenCentre turbine (courtesy of OpenHydro, Ltd.)

(b) Pilot project site and bathymetry

Figure 1 – Case study turbine technology and site

Table 1 – Pilot project turbine parameters

Parameter	Value
Number of turbines	2
Turbine diameter (shroud diameter)	6 m
Water depth	50 - 60 m
Hub height (relative to seabed)	10 m
Efficiency (water-to-wire) (η)	0.33
Cut-in speed ($u_{cut\text{-}in}$)	0.7 m/s
Rated speed (u_{rated})	3.5 m/s

During operation, turbine power output (P) depends on the time-varying inflow velocity (u) as

$$\begin{aligned} P(t) &= 0 && u(t) < u_{cut-in} \\ P(t) &= \frac{1}{2}\rho u(t)^3 A\eta && u_{cut-in} \le u(t) \le u_{rated} \\ P(t) &\approx \frac{1}{2}\rho u_{rated}^3 A\eta && u(t) > u_{cut-in} \end{aligned} \quad (3)$$

where ρ is seawater density (1025 kg/m^3), A is the swept area (defined by the turbine diameter), and η is the water-to-wire power conversion efficiency, assumed to be independent of current velocity. When the inflow velocity is less than the cut-in speed, the turbine does not rotate and no power is generated. Beyond cut-in speed, the power extracted increases with the third power of inflow velocity, until the rated velocity is reached and the extracted power becomes relatively independent of velocity. This is a simplified model for turbine operation that does not account for reduced power output during off-axis flow conditions or velocity-dependent efficiency.

Current velocities at the location of the proposed pilot project have been characterized by bottom-mounted Doppler profilers (Polagye and Thomson, submitted) and are unlikely to exceed the rated speed, as they are designed to operate in more energetic flows. The cumulative probability distributions for inflow velocity and turbine power output at the deployment locations are shown in Figure 2 (B. Polagye, unpublished data). These distributions are derived from one minute ensemble average current velocities at turbine hub height. As discussed in Polagye and Thomson (submitted), this ensemble period includes aspects of both the deterministic and turbulent currents, but does not describe the full range of turbulent motion. Since the responsiveness of tidal turbines to turbulent length and time scales has not been established, the one minute averaging period here is considered sufficient for leading-order analysis.

While operationally significant variations in resource intensity can occur over length scales as short as 100 m in Admiralty Inlet (Polagye and Thomson, submitted), the variation in resource intensity between these two locations is not significant. Consequently, the inflow velocity and power extraction for Turbine 1 is taken as a representative distribution for both turbines.

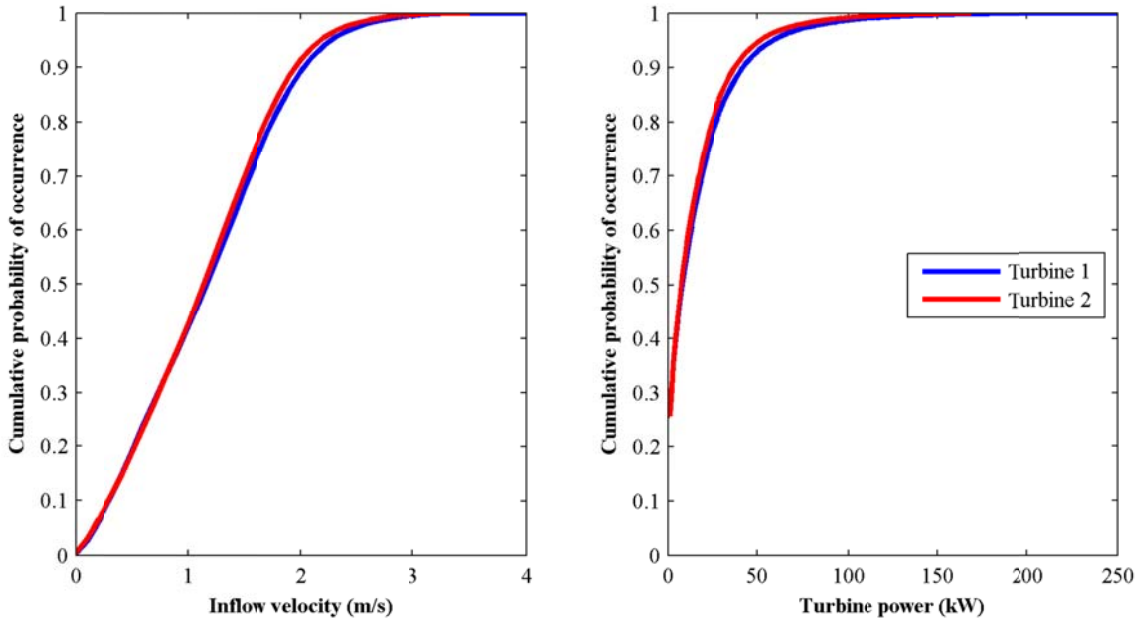

Figure 2 – Cumulative probability distributions for velocity and power output at the deployment locations.

2.2 Tidal Turbine Source Spectrum

To date, there has been no comprehensive characterization of tidal turbine noise. Some acoustic data have been collected (Davidson and Mallows, 2005; Verdant Power, 2010; Ocean Renewable Power Company, 2011), but generally lack context (e.g., quantification of ambient noise in the absence of turbine operation). This limited data set is, in part, attributable to the challenge of collecting acoustic data in such high velocities (Bassett 2010). Here, we present a re-analysis of acoustic data collected from an operating OpenHydro turbine at the European Marine Energy Center (EMEC). Details of prior analyses may be found in Barr (2010) and Polagye et al. (2011b).

2.2.1 Data Collection

Measurements were conducted by the Scottish Association for Marine Science (SAMS) on August 23, 2010. The weather conditions during data collection were wind force 4, Beaufort sea state 3, 0.5 m swell, and raining lightly. The data collection package ("Drifting Ears") consists of an autonomous hydrophone suspended 5 m beneath a surface drogue. The position of the drifter is logged by a GPS on the drogue. The hydrophone records 16-bit sound continuously at 96 kHz. The hydrophone and pre-amplifier has an effective sensitivity of-160 dB re 1 V·µPa and a flat frequency response between 20 Hz and 50 kHz. This customized approach addresses deficiencies in traditional acoustic measurements (e.g., a hydrophone fixed on the seabed or hung from a floating platform) because these expose the hydrophone element to contaminating flow noise from surface friction/turbulence around the element, cable strum, or noise from the seabed mooring. All of these are either non-propagating noise or noise that would not occur in the absence of the measuring device. As tidal energy sites are specifically chosen because of their high flow speeds, these are prime considerations when monitoring ambient sound and device acoustic output. The "Drifting Ears" design maximizes the advantages of recording ambient sound from a drifting platform while minimizing the disadvantages associated with a boat. Turbine parameters during data acquisition included in this analysis are summarized in Table 2. SAMS intended to collect

data over the full range of tidal states and device rotational speeds, but this effort was confounded by high levels of anthropogenic noise from other activities at EMEC (e.g., vessel traffic, commissioning of other turbines). The re-analysis presented here is for measurements at a single turbine operating state (Segment 165b in Figure 3).

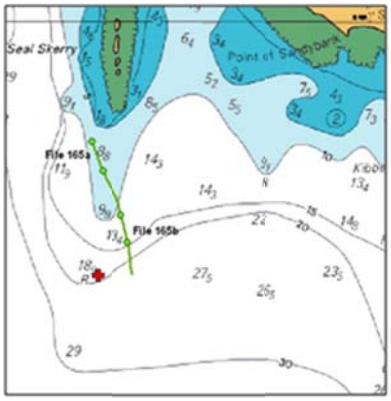

Figure 3 – Drifting hydrophone track. The red cross denotes the location of the OpenHydro turbine.

Table 2 – Turbine parameters during acoustic data collection at EMEC

Parameter	Value
Turbine diameter (shroud diameter)	6 m
Water depth (mean sea level)	15 m
Hub height (relative to seabed)	8 m
Efficiency (water-to-wire) (η)	0.33
Current speed (m/s)	1.8 m/s
Distance to turbine (m)	190-260 m

2.2.2 Source Level – EMEC Turbine (measurement)

For this re-analysis, the manufacturer calibration sensitivity was used to convert the recorded voltage to pressure. This is a simplified approach suitable only for leading order analysis. SAMS field calibrates all drifters using a pistophone and reference hydrophone at the start of a survey, but the data are processed via proprietary format that did not lend itself to our third-party re-analysis. A 64 s recording with the hydrophone in close proximity to the turbine is divided into eight second intervals. Over the eight second interval, the relative separation between turbine and drifting hydrophone is approximately constant. Each interval is analyzed in MATLAB using 2^{16} element windows with 50% overlap and a variance-preserving Hamming filter (Emery and Thomson, 2001). The resulting spectra have low uncertainty (22 degrees of freedom), a bandwidth of 1.5 Hz, and maximum resolvable frequency of 48 kHz (Nyquist frequency).

Figure 4 presents turbine noise recordings in one-third octave sound pressure levels (TOLs)[1]. The recorded turbine noise is "red" with intensity decreasing at ~13 dB/decade. Tonal clusters are apparent around 12.5, 16, 40, 160, 500, and 1600 Hz. The tonal cluster between 12.5 and 16 Hz is consistent with a 10-bladed rotor turning at 12-17 rpm ($f \approx N_{blade}$ x rotational rate), as was the case during this

[1] In presenting this figure, the hydrophone response is assumed to be linear to 10 Hz. The response is only strictly linear to 20 Hz, but, as discussed later in this section, only TOLs with TOB center frequencies of at least 25 Hz are retained in calculating the reference source level. TOLs for received noise below 25 Hz are presented solely to demonstrate the potential for tonal clusters associated with the blade rotation rate.

measurement and higher frequency clusters may be associated with the water-lubricated bearings supporting the rotor cassette. The implication of a relation between the frequency content of turbine noise and turbine rotational rate is discussed further in Sec. 2.4. The tonal peak at 10 000 Hz is not associated with turbine operation, but is rather caused by an acoustic harassment device (seal deterrent) operating at a nearby fish farm (Barr 2010). Since ambient noise profiles were not collected co-temporal with turbine noise, the relative contributions of turbine and ambient noise cannot be readily quantified. Therefore, we conservatively assume that all acoustic energy in the recordings (excepting the 10 000 Hz tonal peak) is attributable to turbine operation. The increase between 10 000 and 30 000 Hz may, however, be associated with rain (e.g., Ma et al., 2005).

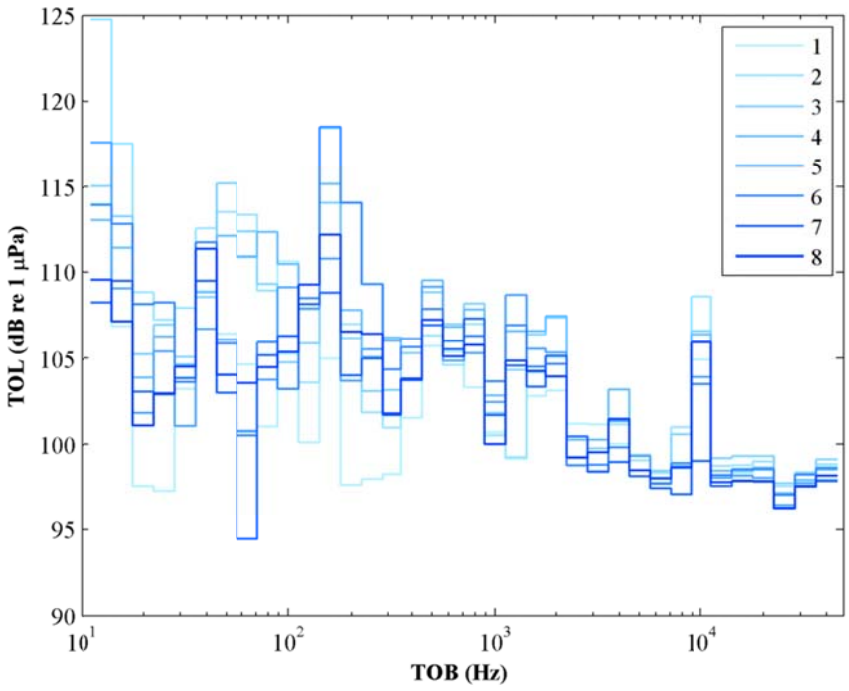

Figure 4 – Received one-third octave sound pressure levels from measurements of an OpenHydro turbine at EMEC.

Source levels in each TOB for each 8 s interval are calculated using the SONAR equation (Urich, 1983)

$$SL = RL + TL \tag{4}$$

where *SL* is the one-third octave source level (dB re 1 µPa at 1 m) (TOL), *RL* is the received level, and *TL* is the transmission loss associated with acoustic spreading and absorption. Acoustic spreading is modeled as spherical propagation (20log*D* transmission loss) within 8 m of the turbine (distance from hub height to water surface and seabed) and cylindrical spreading (10log*D* transmission loss) beyond this distance. Sound absorption is calculated from the frequency-dependent relation given by Anslie and McColm (1998). In equation form,

$$SL(f) = RL(f) + 20\log_{10}(D_s) + 10\log_{10}(D/D_s) + \alpha(f) \tag{5}$$

where *D* is the slant distance between the turbine and drifting hydrophone, D_s is the extent of spherical spreading, and α is the frequency-dependent absorption coefficient. Using logarithm identities, this simplifies to

$$SL(f) = RL(f) + 10\log_{10}(D_s D) + \alpha(f) \ . \quad (6)$$

More complicated descriptions of sound propagation (e.g., Marsh and Shulkin, 1962) are not well-suited for this location given the acoustic reflection from the hard seabed.

The water depth defines the minimum sound frequency ($f_{\text{cut-off}}$) that will freely propagate as (NRC, 2003)

$$f_{cut-off} = \frac{c_w}{4h\sqrt{1-\frac{c_w^2}{c_s^2}}} \quad (7)$$

where h is the water depth and c_s and c_w are the sound propagation speed in the substrate and water, respectively. For hard substrates, the sound propagation speed of the substrate is much greater than water and the denominator asymptotes to $4h$. This suggests a cut-off frequency of ~20 Hz, given a water depth of ~20 m between the source (turbine) and receiver ("Drifting Ears"). Sound at frequencies below the cut-off will continue to propagate, but in a much reduced and site-specific manner (e.g., "hyperspherical" spreading as described by Tougaard et al. 2009). Consequently, we restrict our analysis to TOBs with center frequencies greater than 25 Hz.

Figure 5 shows source spectra for the eight intervals and an average spectrum based on the mean of the rms pressure squared in each third octave band. As observed by McQuinn et al. (2011) this biases the mean towards higher intensity sound and is, therefore, a conservative approach. For both the individual and average spectra, the source level from 7 – 11 kHz has been replaced by a linear decrease (dB/decade) to remove the peak associated with the acoustic harassment device. Given the degrees of freedom in the underlying spectra, the interval variations are attributable to non-stationary noise levels, either because of variations in turbine power output with turbulence (mean flow is quasi-stationary over measurement duration) or fluctuations in ambient noise levels.

The average spectrum is taken as a reference spectrum for turbine noise at a power extraction level corresponding to an inflow velocity of 1.8 m/s and water-to-wire efficiency of 33%.

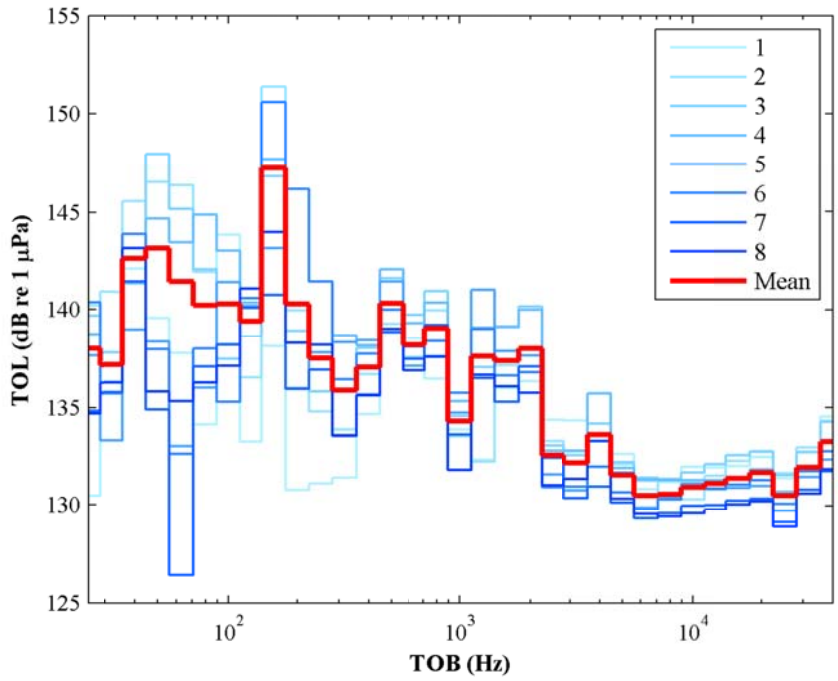

Figure 5 – One-third octave source levels from measurements of an OpenHydro turbine at EMEC (acoustic harassment device removed by linear interpolation).

2.2.3 Source Level – Admiralty Inlet Case Study (estimate)

The reference spectrum from measured data at EMEC corresponds to a specific power generation state. During the case study deployment, the turbine would encounter a wide range of inflow velocities. A simple scaling relation is needed to extrapolate the reference spectrum to a similar device operating under different inflow conditions. We proceed under the assumption that the acoustic power output from an operating tidal turbine should vary with inflow velocity, for example, due to variations in the strength of the shed vortices. Davidson and Mallows (2005) encountered a similar problem in making a pre-installation estimate for the Marine Current Turbine (MCT) SeaGen on the basis of a smaller turbine, the MCT SeaFlow. Their assessment utilized Hazelwood and Connelly's (2005) empirical result that the acoustic pressure from underwater noise generated by mechanical processes scaled with the mechanical power input. Davidson and Mallows hypothesized that this relation could be extended to turbine power generation and their pre-installation estimate was in general agreement with post-installation acoustic monitoring. However, no peer-reviewed work has rigorously assessed this relation and further work to verify its accuracy is a recommended next step.

Here, we accept Davidson and Mallows' (2005) hypothesis regarding turbine noise and extend it to estimate the probability distribution of turbine noise for the expected distribution of power generation states. As mentioned previously, inflow conditions for Turbine 1 (Figure 2) are taken to be representative of the inflow conditions for both turbines. A strong caveat to this approach is that the data obtained from turbine operation at EMEC suggests that the frequency content of the noise generated by a tidal turbine is, at least in part, related to its rotational rate. Consequently, the frequency content of the noise would be expected to vary with inflow condition (for a device operating at constant tip-speed ratio). In other words, both the intensity *and* frequency content of turbine operating noise

may vary with inflow condition. To proceed with this thought exercise, by necessity, we assume that the frequency content *does not* vary with inflow condition (Sec. 2.4 contains further discussion on the implications of this assumption).

If the source level for a specific frequency at a reference power generation state (P_0) is related to the acoustic pressure (p_o) at this state by

$$SL(f, P_0) = 10 \log\left(\frac{p_0^2}{p_{ref}^2}\right) \qquad \text{(dB re } p_{ref} \text{ at 1 m)}, \tag{8}$$

then, based on Hazelwood and Connelly (2005), the source level for a similar turbine at a different power generation state would be given by

$$SL(f, P) = SL_0(f, P_0) + 10 \log\left(\frac{P^2}{P_0^2}\right) \tag{9}$$

where P is given by (3) as a function of inflow velocity and turbine specifications (e.g., efficiency, cut-in speed). Since the swept area and efficiency of the turbine monitored at EMEC are identical for the turbines proposed for Puget Sound, substituting (3) into (9) and simplifying terms yields

$$SL(f, P) = SL_0(f, P) + 10 \log\left(\frac{u^6}{u_0^6}\right) \tag{10}$$

where u_0 is the inflow velocity and turbine efficiency during the reference measurements (here, measurements at EMEC). Equation (10) suggests that the source level for a tidal turbine should be a strong function of inflow velocity. The sixth power dependency of noise on inflow velocity implies a corresponding dependency on rotational rate for a device operating at constant tip-speed ratio. This is consistent with literature on a fan noise (Barber 1992, Chap. 4) as the broadband acoustic power generated by a fan varies, empirically, with the fifth to sixth power of rotational rate.

Below cut-in speed, when the turbine would rotate, noise from the flow around the support structure and stationary rotor is unlikely to be detectable at a significant distance (Polagye et al. 2011a, Sec. 3.4). In other words, $SL(f,0) = 0$.

2.3 Characteristics of Ambient Noise in Admiralty Inlet

Pre-installation site characterization studies for the proposed pilot project have included long-term, low-duty cycle ambient noise measurements using an autonomous hydrophone on the seabed, as described in Bassett et al. (2010), Bassett et al. (submitted), and Bassett et al. (in prep). The measurement system consists of a self-contained data acquisition and storage system (Loggerhead Instruments DSG) with a hydrophone (HTI-96-Min) and internal preamplier. The hydrophone has an effective sensitivity of -165.5 dB re 1µPa V^{-1}. The frequency response of the hydrophone and data acquisition system is flat (± 3 dB) from 20 Hz to 30 kHz. Digitized 16-bit data are written to a SD card.

For the purposes of this analysis, ambient noise is partitioned into a low frequency component (f < 1000 Hz) and high-frequency component (f > 1000 Hz). In the low frequency regime, ambient noise is independent of inflow velocity, but ambient noise is correlated with inflow velocity at higher frequencies. The contributions of various sources to the ambient noise budget are visualized in Figure 6 in a manner similar to the classic “Wenz” curves describing ocean noise (Wenz, 1962).

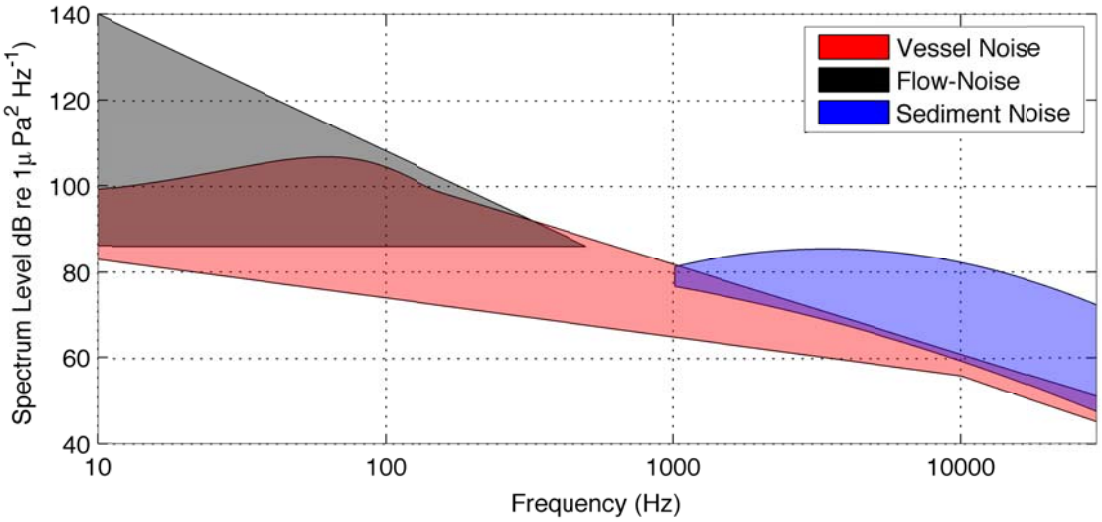

Figure 6 – Relative intensity and distribution of noise sources associated with strong tidal currents.

2.3.1 Low Frequency Ambient Noise (25 Hz – 1000 Hz)

As demonstrated in Bassett et al. (submitted), ambient noise in northern Admiralty Inlet, particularly at frequencies below 1000 Hz, are dominated by vessel traffic and are insensitive to spatial position over length scales on the order of 1-2 km. This is attributed to a traffic separation zone that forces the majority of vessel traffic to follow a regular pattern while transiting the inlet. Percentile pressure spectral densities are reproduced from this work in Figure 7. These statistics exclude periods with depth-averaged currents greater than 0.4 m/s to avoid bias from non-propagating pseudo-sound. During intense tidal currents, the turbulent eddies shed by the hydrophone element give rise to high-intensity pseudo-sound at frequencies up to 750 Hz (range of affected frequencies corresponds to the extent of the inertial subrange) (Bassett et al., in prep). This sound is non-propagating and is not appropriately included in an ambient noise budget (Polagye et al. 2011a, Sec 3.4). In this frequency regime (25 Hz – 1000 Hz), tidal currents do not generate propagating sound and, therefore, ambient noise and tidal current noise are uncorrelated. In other words, over time, all ambient noise states are equally probable for turbine power generation states. Turbine noise in this frequency band is similar to the ambient noise distribution, excepting the tonal peaks previously discussed (e.g., relative peak at 160 Hz).

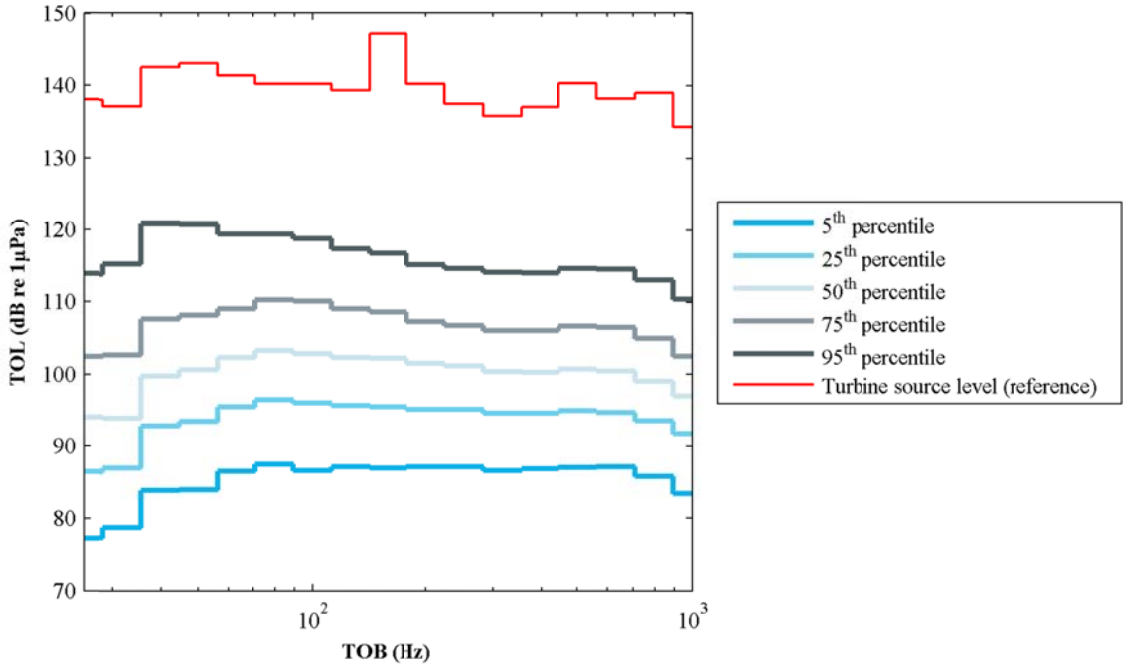

Figure 7 – Percentile TOLs for ambient noise (25 – 1000 Hz)

2.3.2 High Frequency Ambient Noise (1000 Hz – 25 000 Hz)

Strong currents mobilize sediments on the seabed (in this case, gravel and shell hash mixed amongst the predominant cobble overburden). This generates propagating noise at frequencies greater than 1000 Hz, with intensity dependent upon current velocity, as shown in Figure 6. Vessel traffic, breaking waves, and precipitation also contribute to the ambient noise budget, but, particularly during periods of strong currents are dominated by bedload transport (Bassett et al., in prep). Therefore, at these frequencies noise generated by the turbine is correlated with ambient noise.

The same underlying dataset as for low-frequency ambient noise is again used, but for the high-frequency analysis, measurements at all velocities are retained and ambient noise distributions are stratified by hub-height velocity. Median TOLs as a function of velocity are presented in Figure 8 and show a clear increase in median TOLs as a function of velocity, most pronounced for TOBs with center frequencies greater than 4 kHz.

Turbine noise is relatively flat in this frequency regime. It should, however, be noted that the spectrum of turbine noise, particularly at frequencies exceeding 6000 Hz closely resembles the ambient noise spectrum from Admiralty Inlet when hub height velocities would be 2.0±0.2 m/s. Since turbine noise data were collected in a similar current regime (hub height velocity ~1.8 m/s), it is possible that the reference spectrum of "turbine noise" at this frequency is, in fact, bedload transport at the EMEC site. If this is the case, turbine noise would be biased relative to ambient in these frequencies, since source levels are estimated to scale with the sixth power of current velocity, while Bassett et al. (in prep) indicates that bedload transport noise scales with the square of current velocity.

The tonal peak in ambient noise data at 1500 Hz is likely an artifact of coherent sound reflection from the seafloor. Sound pressure levels at this frequency are consistently 6 dB greater than surrounding

frequencies (consistent with coherent addition) and the separation between hydrophone and the seabed is 1 m, corresponding to a frequency of 1500 Hz in seawater.

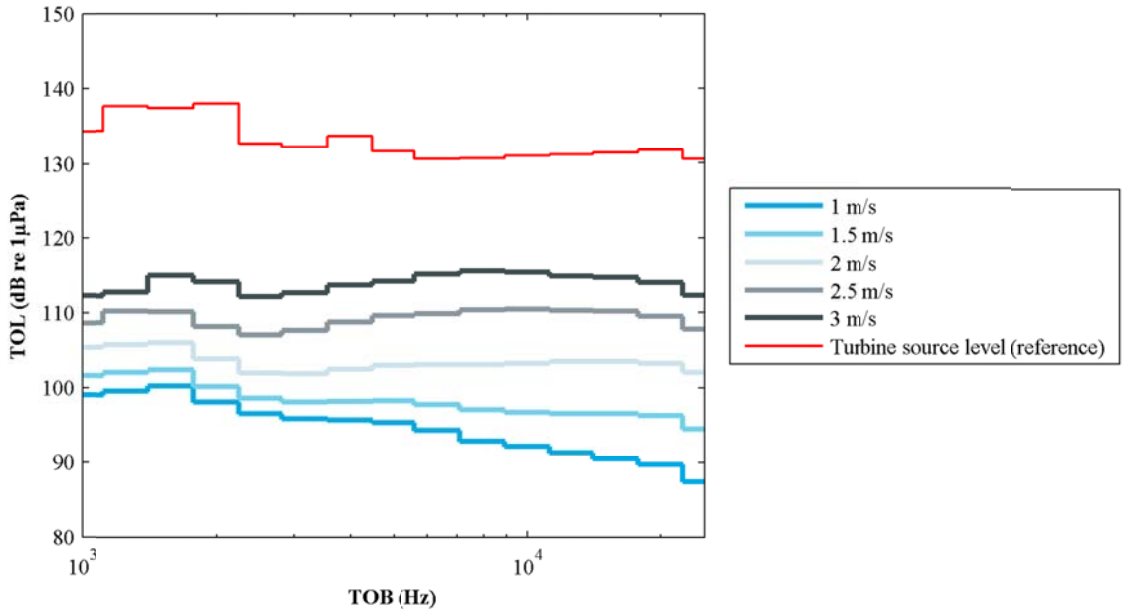

Figure 8 – Median TOLs for ambient noise as a function of velocity (1000 – 25 000 Hz)

2.4 Detection of Turbine Noise Relative to Ambient Noise

As described in the introduction, the effect of turbine noise relative to other sources of ambient noise is quantified in terms of the "signal excess" (NRC, 2003)

$$SE = RL - NL = SL - TL + AG - NL$$

where *SE* is the signal excess, *RL* is the received level, *SL* is the source level, *TL* is the transmission loss, *AG* is the auditory gain of the receiver (i.e., signal processing, either computational or biological), and *NL* is the noise level. All of these terms are frequency dependent (in this case study, represented by one-third octave bands). The signal excess must also be considered in terms of receiver hearing thresholds. Specifically, if, for some distance from the turbines and power generation state, a TOL is less than the hearing threshold for the receiver in that TOB, the noise from the turbines will not be detected, regardless of ambient noise level. *SE* for a receiver is, therefore, given by

$$SE = \max(RL, 0) \qquad RL \geq HT \tag{11}$$

$$SE = 0 \qquad RL < HT \tag{12}$$

where *HT* is the hearing threshold of the receiver. In other words, this representation of *SE* is always non-negative. A positive signal excess denotes detection of sound by a receiver.

Noise levels (*NL*) for the case study site are as presented in Sec. 2.3. The frequency space for this analysis span the three decades from 25 Hz to 25 000 Hz and is separated into low-frequency and high-frequency regimes at 1000 Hz. The lower limit is set by the lowest resolvable frequency for characterized turbine noise, while the upper limit corresponds to the highest frequency for which ambient noise has been characterized at the case study site.

In the follow sub-sections, the model for received levels is described, followed by a discussion of *AG* and *HT* associated with specific study objectives. Before proceeding, we note, again, the assumption that the frequency content of turbine noise is independent of flow velocity. However, since the ambient noise probability distribution by one-third octave band changes slowly, this is a reasonable simplifying assumption for this case study.

2.4.1 Received Level Model

As described by (10), the turbine source levels are expected to vary with inflow velocity. Received levels at a slant distance (*D*) from the turbine are modeled using the SONAR equation as

$$RL(f,P) = SL(f,P) - 20\log_{10}(D) - \alpha(f)D \qquad D \le D_s \tag{13}$$

$$RL(f,P) = SL(f,P) - 10\log_{10}(DD_s) - \alpha(f)D \qquad D > D_s \tag{14}$$

where D_s is the transition from spherical to cylindrical spreading. For the case study site, D_s is assumed to be 30 m, based on a hub height of 10 m in 55 m of water. Because received levels depend logarithmically on D_s, results are relatively insensitive to perturbations about this assumed value. This is also results in sound propagation consistent with the practical spreading (15log*D* for all *D*) reported by Bassett et al. (submitted) for vessel traffic noise at this location to a range of 5 km. As demonstrated in Sec. 2.3, the frequencies of interest for tidal turbine noise and vessel traffic noise are similar.

Received levels for the pair of turbines are calculated using MATLAB (www.mathworks.com) on a two-dimensional grid with a horizontal resolution of 10 m. The grid is positioned 30 m below the water surface at nominal mid-water for the case study site. The grid extent is 5000 m in each horizontal dimension. Turbines are positioned at [x,y,*z*] coordinates [35 m, 2 m, -45 m] and [-35 m, -2 m, -45 m] (z = 0 corresponds to the surface, downward negative). The sound generated by each turbine is assumed to be incoherent, such that the total acoustic pressure (p_{total}) at a grid node is given by

$$p_{total} = \left(p_1^2 + p_2^2\right)^{1/2}. \tag{15}$$

These two pressures are, in general, unequal, because of the differences in distance between a grid node and each source. In terms of the received levels calculated by (13) or (14)

$$RL_{x,y,z}(f,P) = 10\log_{10}\left(10^{RL^1_{x,y,z}/10} + 10^{RL^2_{x,y,z}/10}\right). \tag{16}$$

For each TOB, received levels at all grid points are calculated for integer TOL source levels (i.e., …135 dB, 136 dB,…). In doing so, it is assumed that the source levels for both turbines will be nearly equal at any instant in time (supported by turbine proximity and similar velocity distributions). A probability distribution of received levels at a grid point is obtained by combining the calculated received levels with the probability distribution for turbine source levels.

This is a simplified approach to modeling received levels. It assumes that the sound from turbines is omnidirectional and parameterizes the effect of the acoustic waveguide (surface, seabed) in a way that neglects the potential for interference patterns or the effect of the headland. As established in the introduction, our objective is not a comprehensive treatment of turbine noise, but rather to advance an approach for probabilistic assessment of noise that can inform monitoring study design. For this purpose, the simplified model provides instructive guidance.

2.4.2 Characterization of Turbine Noise by a Hydrophone

For turbine noise characterization studies, the receiver will most likely be a hydrophone (or hydrophone array) either deployed from a surface vessel or drogue (e.g., "Drifting Ears") in order to minimize contamination by pseudo-noise during strong currents. It may also be possible to use stationary hydrophones equipped with flow shields (Lee et al., 2011). A properly specified hydrophone will be equally sensitive to all frequencies of interest and, therefore, $HT(f)$ is assumed to be +0 dB for all frequencies. Our experience with noise characterization at this location suggests that accurate quantification of turbine noise relative to other ambient sources with similar frequency distribution will likely require a signal excess of at least +5 dB, assuming no auditory gain through signal processing algorithms (AG = +0 dB). The detectability of turbine noise in a TOB, therefore, requires $SE \geq +5$ dB.

2.4.3 Marine Animal Responsiveness to Turbine Noise

The objective of marine mammal monitoring studies is to identify potential behavioral responses to the noise generated by operating turbines. In this case, the receiver is biological and the signal excess for detection/behavioral change depends on both species and frequency band.

Aquatic species have evolved to detect conspecific signals in noisy environments. For example, Miller (2006) chose AG = +6 dB to evaluate killer whale active space. However, hearing mechanisms are not likely to have evolved to detect increased anthropogenic noise relative to similar background ambient noise. Therefore, signal processing capabilities are likely to be less sensitive for turbine noise than for conspecific calls and we assume that AG = +0 dB for biological receivers. We also assume that marine animal hearing is unlikely to be affected by pseudo-noise, regardless of relative motion between currents and the animal.

For biological receivers, we select four species for which hearing thresholds are relatively well understood to represent classes of marine animals. For each representative species, signal excess over the study area are considered for six one-third octave bands (50 Hz, 160 Hz, 500 Hz, 2000 Hz, 8000 Hz, and 25 000 Hz). The first four TOBs correspond to relative amplitude peaks in the turbine source spectrum (i.e., frequencies with the highest expected signal to noise ratio at the case study site). Note, also, that this excludes from analysis the artifact in ambient noise at 1500 Hz. These are also frequencies for which ambient noise will be uncorrelated with turbine noise. The latter two frequencies correspond to important frequencies for marine mammal communication where ambient noise and turbine noise are correlated. Several caveats are required regarding uncertainty in the results. First, auditory response data is limited for all aquatic species and the hearing thresholds presented in Table 3 are often for one individual and may not be representative of the species as a whole. Second, since hearing thresholds for low-frequency cetaceans are not available (Southall et al., 2007), this analysis excludes an entire class of cetaceans that may be infrequently present in the case study area (Snohomish PUD, 2009). Detection of turbine noise by low-frequency cetaceans is, however, discussed qualitatively in Sec. 4, following presentation and discussion of quantitative results for other species. Diving birds might also be exposed to turbine noise (Polagye et al. 2011a, Sec. 4.6), but their auditory responsiveness is even less well understood than low-frequency cetaceans and they are not included in the discussion. Third, as previously discussed "turbine noise" at 8000 and 25 000 Hz may actually be bedload transport.

Table 3 – Hearing thresholds (*HT*) for representative species (∞ denotes no auditory responsiveness in this TOB)

	TOB Center Frequency (Hz)	**50**	**160**	**500**	**2000**	**8000**	**25 000**
Class	**Representative Species**						
Fish (hearing generalists)	Atlantic cod (*Gadus morhua)* (Popper and Hastings, 2009)	82	74	107	∞	∞	∞
Mid-frequency cetaceans	Killer whale (*Orcinus orca)* (Wartzok and Ketten, 1999)	∞	120	100	98	55	37
High-frequency cetaceans	Harbor porpoise (*Phocoena phocoena*) (Kastelein et al., 2002)	∞	∞	90	70	58	38
Pinnipeds	Harbor seal (*Phoca vitulina*) (Kastak and Schusterman, 1998; Terhune 1988)	∞	106	88	67	58	64

The detection of sound by biological receivers is a necessary, but not sufficient, condition for behavioral response and, therefore, a conservative estimate for the probability of observing a behavioral response (Richardson et al., 1995; Southall et al., 2007).

2.4.4 Warning Distance

While noise from turbines is generally discussed in the context of potential environmental impacts, the noise turbines generate also provides an important cue to alert marine animals to the presence of the device, as first considered by Carter (2007). Awareness of an operating turbine provides the opportunity for a marine animal to avoid potentially more significant risks, such as entanglement, collision, or blade strike. For a turbine with a constant tip-speed ratio, the significance of interactions, such as blade strike, increases with current speed. While detection of the "bow wake" upstream of the turbine, echolocation, and visual detection are also possible mechanisms by which marine animals might become aware of the turbine, noise is expected to be the leading detection mechanism. Carter's (2007) analysis was subject to high uncertainty in both received levels and ambient noise levels and predicted warning times ranging from minutes to less than a second, depending on the assumptions made. Therefore, it is instructive to revisit this question with improved information. In the present analysis, the "Warning Distance" is defined as the minimum distance from the turbine at which positive signal excess occurs at some percentile ambient noise level. These are evaluated for the one-third octave bands described above and presented as a function of turbine inflow velocity and species class.

3 Results

3.1 Probability Distribution of Turbine Source Levels

Given the probability distribution of inflow velocities given in Figure 2 and turbine design parameters in Table 1, application of (7) yields the distribution of turbine source levels shown in Figure 9. The maximum broadband (25 - 25 000 Hz) source level is estimated to be 172 dB re 1µPa at 1m,

corresponding to an inflow velocity of 3.6 m/s. This source level will occur infrequently during turbine operation (< 0.01% of time) and represents a considerable extrapolation from reference measurements. Received levels are, therefore, never expected to rise to a level that would be categorized as injurious (e.g., permanent threshold shifts) at this location (180 dB re 1µPa, Southall et al., 2007). Likewise, predictions of low intensity sound at periods around cut-in speed (common occurrence) are also subject to high uncertainty.

Broadband received levels in the vicinity of the project for four inflow velocities are shown in Figure 10. The interaction between the two sources is only apparent at close range (e.g., within 100 m). At more distant locations, received levels are indistinguishable from those associated with a single point source. The dashed black contours denote the 120 dB isobel, the current regulatory threshold for harassment of marine mammals (Southall et al, 2007). This supports introductory assertion that the acoustic effects of pilot-scale projects are unlikely to rise to the level of acoustic impacts.

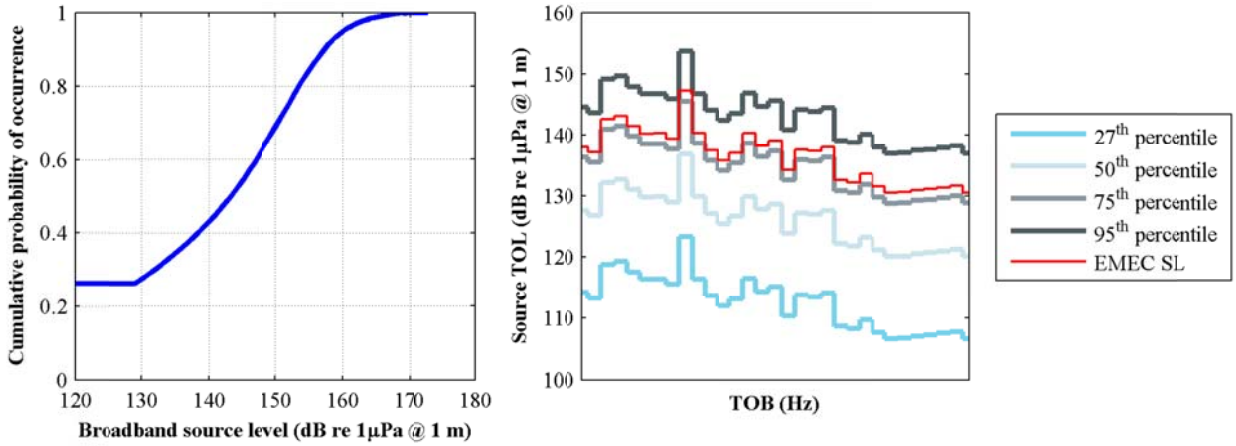

Figure 9 – Probability distribution of turbine source levels. (left) Broadband (25 – 25 000 Hz). (right) One-third octave source levels for select percentiles. Turbine operation begins at the 27th percentile currents. The red line denotes the turbine source level estimated from measurements at EMEC.

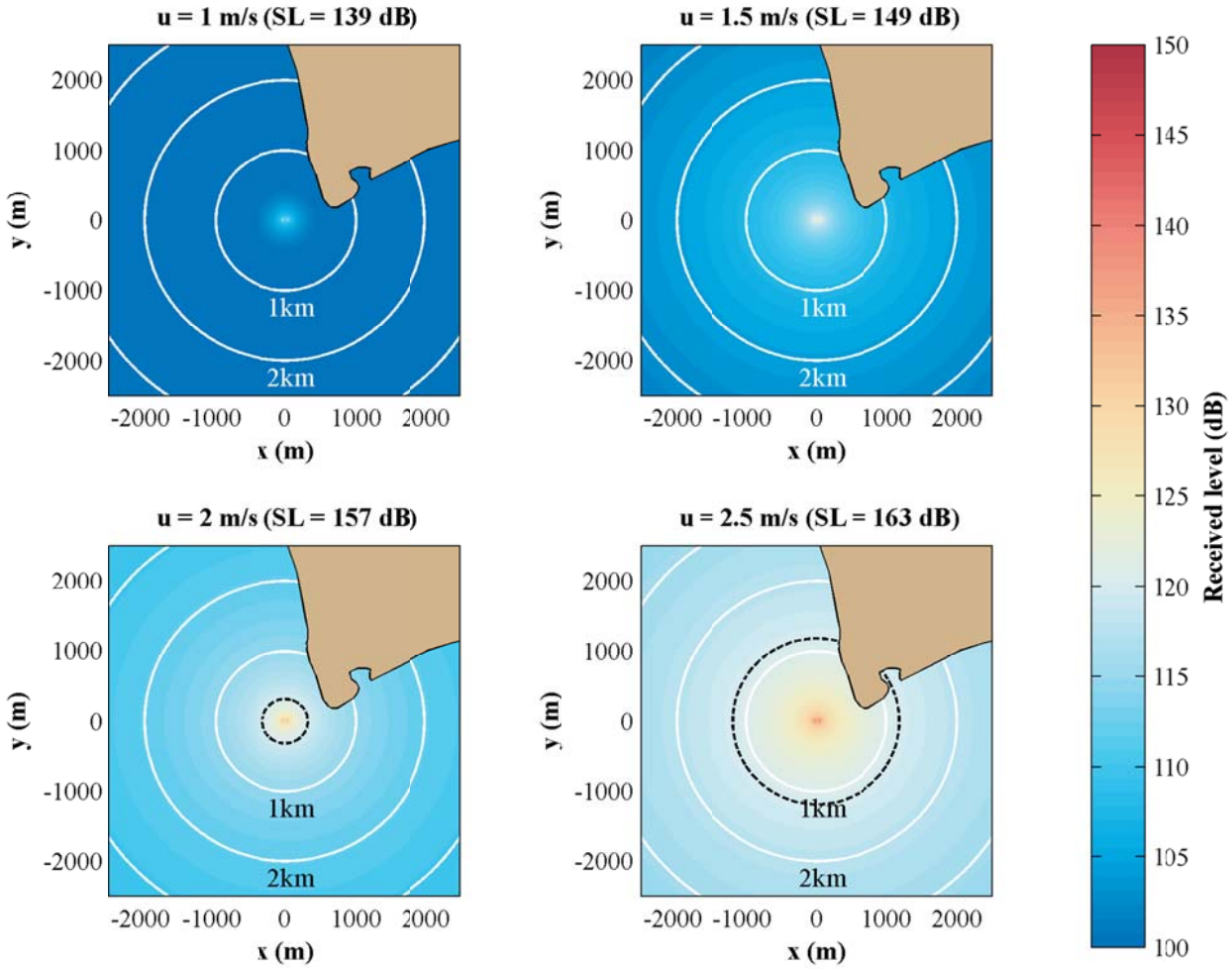

Figure 10 – Broadband (25 - 25 000 Hz) received levels at four inflow velocities (30 m depth relative to surface). Dashed black contour denotes the 120 dB isobel (regulatory harassment threshold at this site).

3.2 Effectiveness of Studies to Characterize Turbine Noise

Characterization of turbine noise over a range of inflow velocities will be required in order to verify or disprove Davidson and Mallows' (2005) hypothesis regarding the correlation of turbine noise and power generation state. To assess the effectiveness of studies targeted towards this goal, detection statistics for a set of representative inflow velocities (1.0, 1.5, 2.0 and 2.5 m/s) will be needed. Specifically, Figure 11 shows the percentage of TOBs (25 Hz – 25 000 Hz) in which the probability of detecting turbine noise is greater than 75% with the hydrophone parameters previously outlined ($SE \geq +5$dB, $AG = 0$ dB, $HT = 0$ dB). Results suggest that it will be difficult to characterize turbine noise across a majority of one-third octave bands when currents are lower than 2 m/s and then, only at relatively close range (< 1 km).

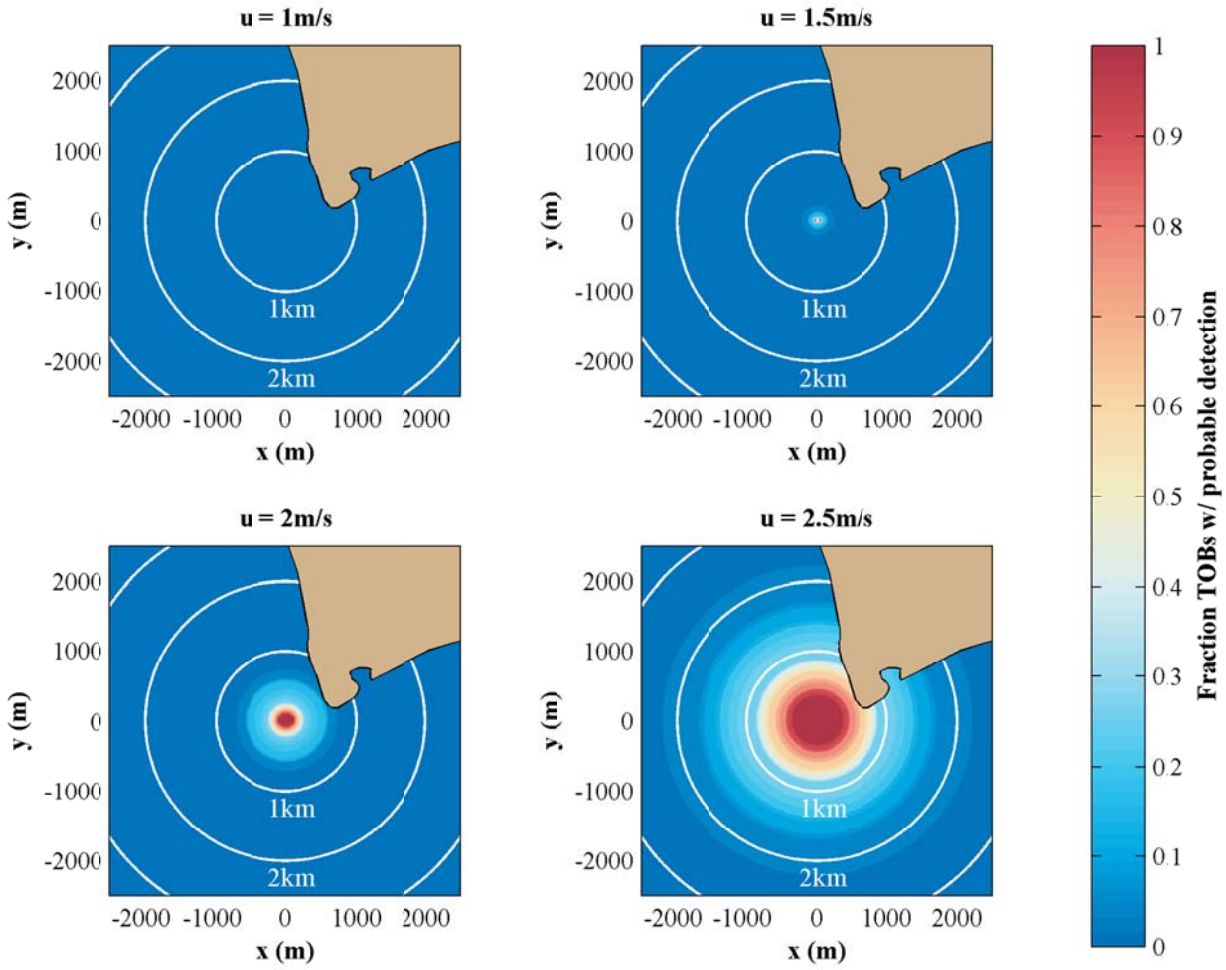

Figure 11 – Percentage of one-third octave bands detected relative to ambient noise (at least 75% probability, 25 – 25 000 Hz) at four inflow velocities (30 m depth relative to surface).

3.3 Effectiveness of Studies to Monitor Animal Responsiveness to Turbine Noise

Studies to evaluate the behavioral response of marine animal responsiveness to turbine noise are structured to improve the understanding of whether turbine noise is likely to cause behavioral changes (e.g., changes in diving behavior, attraction, avoidance). Because behavioral response is not uniquely determined by received noise levels, but are rather a complicated function of behavioral state, direction of motion relative to the source of the sound, and the individual experiences of a marine animal (Wartzok et al., 2003; Southall et al., 2007; Ellison et al., 2011), we have chosen to focus on the detection of turbine noise. Because the zone of responsiveness cannot exceed the zone of detection (Richardson et al., 1995), the spatial extent over which sound could be detected by different classes of marine animals provides the maximum spatial extent of a survey area that needs to be monitored for behavioral responses (i.e., marine animals cannot respond to sound they cannot detect).

As discussed in Sec. 2.4.3, four representative species are used to describe fish, mid-frequency cetaceans, high-frequency cetaceans, and pinnipeds. The probability of turbine noise detection for these classes of marine animal are summarized in Figure 12 – Figure 15 in one-third octave bands corresponding to relative peaks in turbine noise, or important communication frequencies. The

presented figures show the probability of detecting turbine noise at some distance from the turbine over the joint distribution of power generation states and ambient noise. Because turbines are not expected to generate significant noise while idle, the maximum possible detection probability corresponds to the percentage of time the turbines are expected to operate (73%).

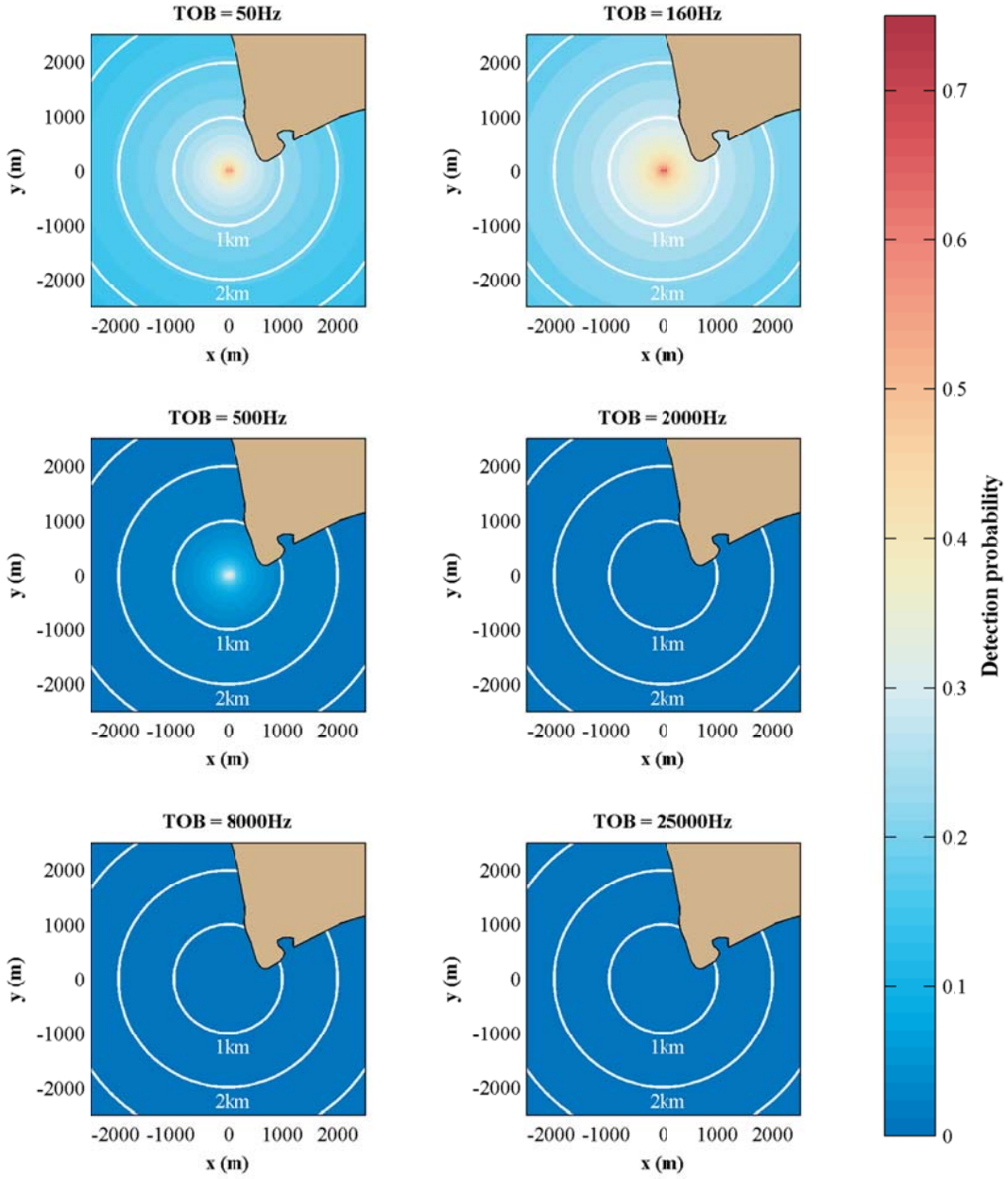

Figure 12 – Probability of fish (Atlantic cod, hearing generalist) detecting turbine noise (30 m depth relative to surface).

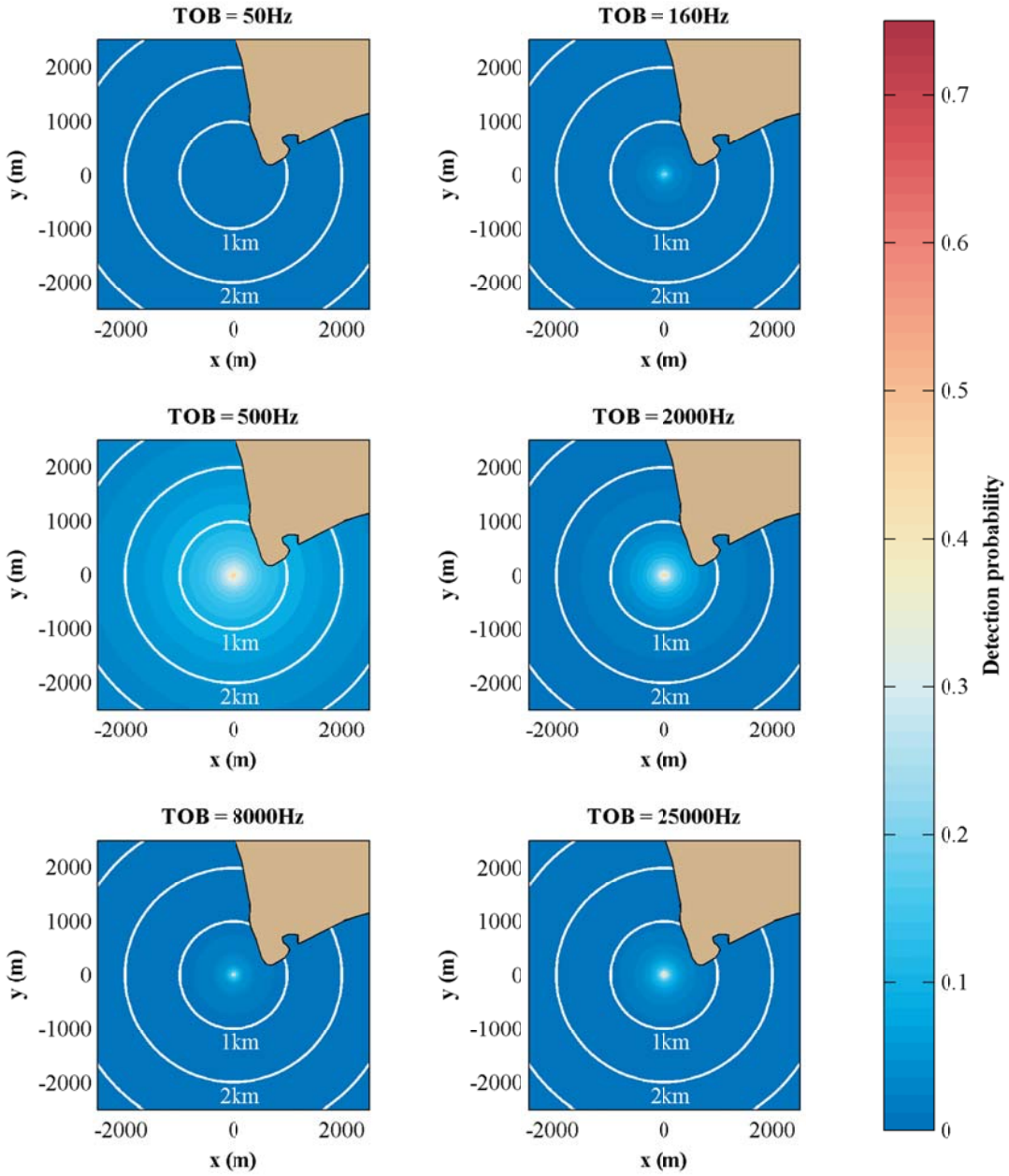

Figure 13 – Probability of mid-frequency cetacean (killer whale) detecting turbine noise (30 m depth relative to surface).

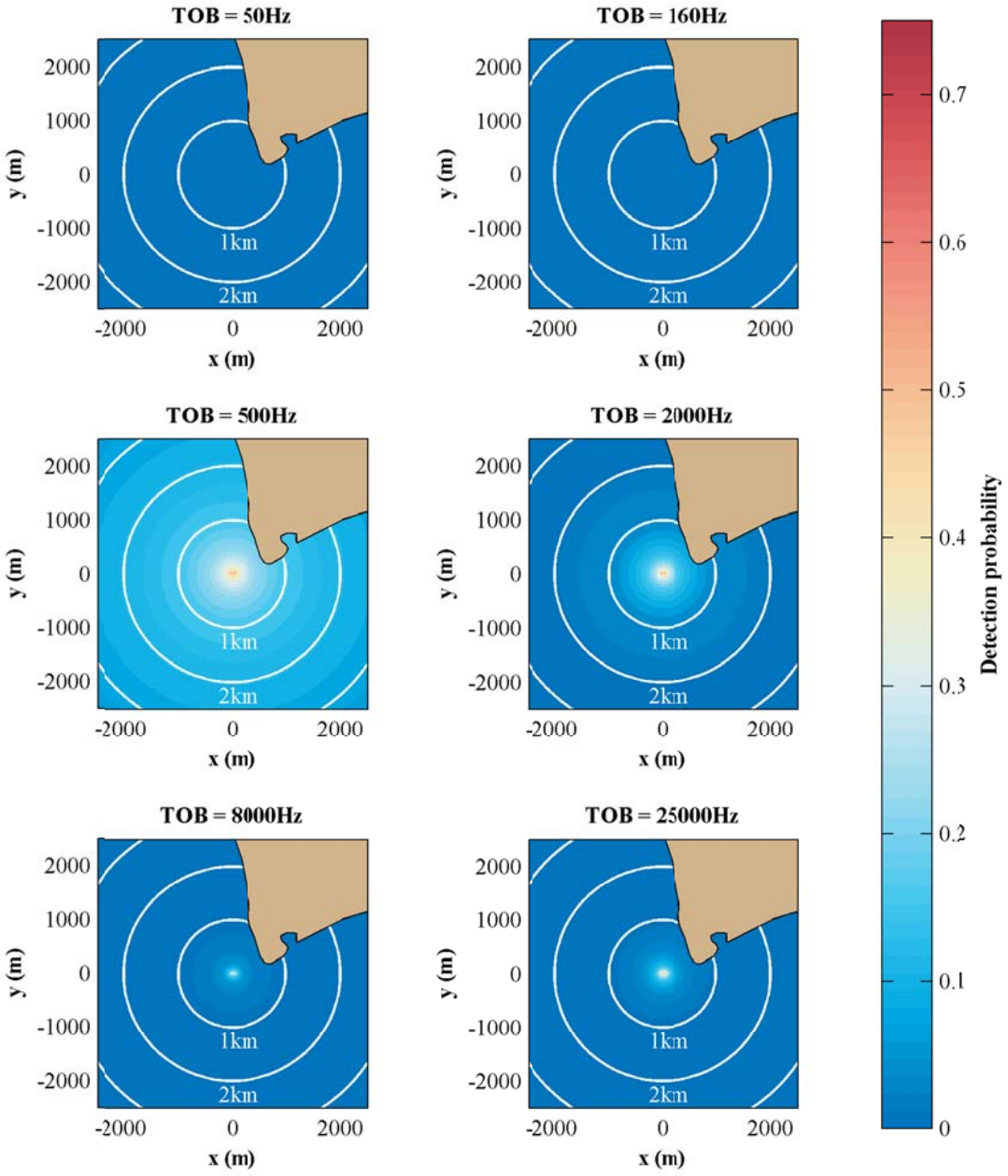

Figure 14 – Probability of high-frequency cetacean (harbor porpoise) detecting turbine noise (30 m depth relative to surface).

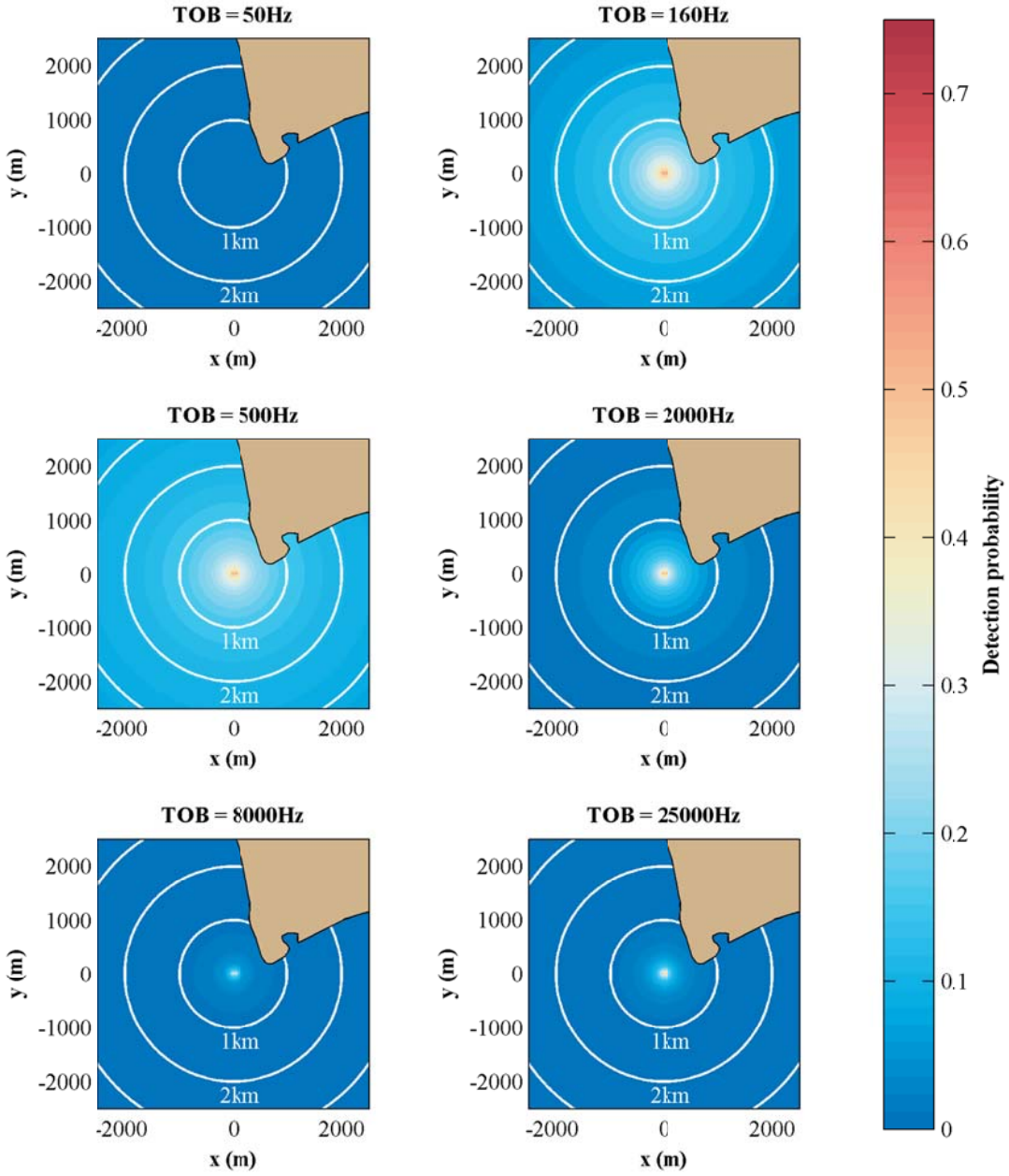

Figure 15 – Probability of pinniped (harbor seal) detecting turbine noise (30 m depth relative to surface).
For all marine mammal classes considered, detection probabilities drop below 50% within a few hundred meters of the turbines and often drop below 25% within a kilometer. Detection probabilities are similar for all classes above 500 Hz. Pinnipeds are likely to detect noise at lower frequencies, as well (i.e., 160 Hz). While the signal excess in this band is greater than for higher frequencies, the hearing thresholds for mid- and high-frequency cetaceans limits their capabilities to detect it. Fish, while unable to detect high frequency noise from the turbines (i.e., at frequencies greater than 500 Hz) are able to detect lower frequency noise over a broader spatial extent than marine mammals.

3.4 Warning Distance

Warning distances, the minimum distance from either turbine to 100% detection probability, are shown for 5th, 50th, and 95th ambient noise probability distributions in Figure 16. During the quietest periods, turbine noise will be audible to a range of several hundred meters during most power generation states. During the loudest periods, turbine noise would not be detectable at close range (i.e., < 10 m) during weak currents and would only be detectable at significant range for some receivers once currents exceed 2 m/s. For median ambient noise conditions, warning distances are typically at least 50 m during weak currents and several hundred meters during strong currents.

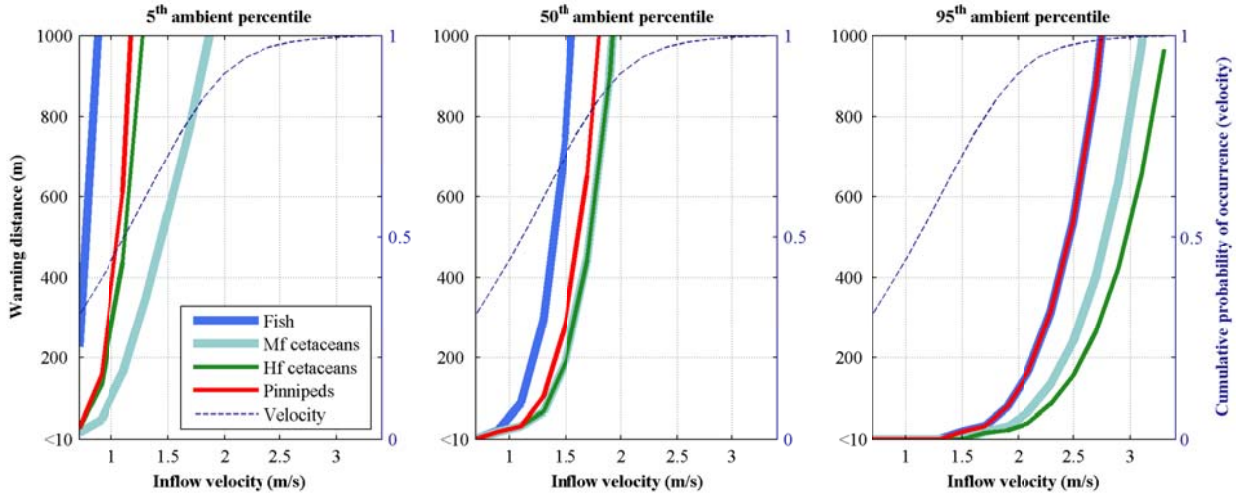

Figure 16 – Warning distance (30 m depth relative to surface) as a function of inflow velocity.

4 Discussion

4.1 Monitoring Effectiveness

For this case study, the spatial extent of detectable turbine noise in the one-third octave bands considered is quite limited in comparison to the spatial extent of northern Admiralty Inlet. The inlet is approximately 5000 m wide at the narrowest location between Point Wilson and Admiralty Head. By comparison, with a few hundred meters of the turbines, the probability of turbine noise exceeding ambient levels drops below 50%. This has a number of implications for the effectiveness of post-installation monitoring plans.

A significant uncertainty in this pre-installation case study is the relation between turbine noise (intensity and frequency) and power generation state. Here, we have applied Davidson and Mallows' (2005) hypothesis that rms pressure will vary with the power extracted and results show a strong dependence on current velocity. Developing accurate, data-driven expressions for this relation is a critical research need. As shown by Figure 11, if Davidson and Mallows ' hypothesis is correct, characterizing turbine noise at this location is predicted to be difficult for inflow velocities less than 2 m/s, while currents at or above 2 m/s occur only 20% of the time (Figure 2). Further, if the objective is to estimate the source level based on a regression through measurements at multiple distances (as could be accomplished through simultaneous deployment of multiple drifting hydrophones), the confidence intervals on the regressed source levels will be broad for the majority of inflow conditions (i.e., turbine noise is only detectable at limited distances under the most common operating conditions). At this site,

study effectiveness can be improved by collecting data at times when ambient noise is known to be low, such as the early morning hours (0200 – 0500 local time when shipping traffic is at its daily minimum, Bassett et al. submitted). However, peak tidal currents and acceptable weather may not routinely coincide with minimal ambient noise conditions.

Similar considerations apply to monitoring marine animal responsiveness to turbine noise. The pre-installation case study presented here suggests that observations should be stratified by current velocity and focused on the immediate vicinity of the turbines (e.g., no more than few hundred meters) or restricted to periods in which turbine noise is likely to be detectable over a larger area. Both of these limitations could potentially decrease the sample size for observations and erode statistical power to detect change, particularly for marine mammals which are only occasionally present in the project area (e.g., endangered Southern Resident killer whales). Shoreline observers using a combination of theodolite and video camera should, however, be able to achieve meter-scale accuracy (Denardo et al., 2001), enabling a fine spatial stratification for observations. Observers will not, however, be able to routinely take advantage of known low-ambient noise periods at this site given the lack of ambient light for visual-spectrum observations during these periods (0200-0500 local time) and the limited resolution of the current generation of infrared detectors (Graber et al., 2011).

In Admiralty Inlet, with water depths exceeding 60 m, the low-frequency propagation cut-off is less than 10 Hz (6). As observed from the measurements at EMEC, turbines noise is likely to have a tonal cluster at frequencies below the 25 Hz limit considered in this analysis. Ambient noise levels are lower at these frequencies for the case study site (Bassett et al., submitted) and low-frequency cetacean hearing in these frequencies is likely evolved to be more sensitive than fish hearing. Consequently, low-frequency cetaceans may detect turbine noise at greater distances than medium-frequency cetaceans, high-frequency cetaceans, pinnipeds, or fish, making them a potentially interesting indicator species. However, low-frequency cetaceans are not common in Admiralty Inlet (several transits per year, Snohomish PUD, 2009) which will limit the statistical power of studies to detect behavioral changes.

Click detectors are increasingly popular passive acoustic tools for studying the responsiveness of high-frequency cetaceans (e.g., harbor porpoise) to offshore activities. For example, click detectors have been used successfully to monitor the response of harbor porpoise to pile driving for offshore wind farm installations (Tougaard et al. 2009).These autonomous hydrophones log information about echolocation click trains and can be used to assess trends in presence/absence of marine mammals. Click detectors have been deployed at the case study site to establish baseline harbor porpoise activity (Cavagnaro et al., in prep) and could be used for before and after comparison. However, in the frequencies of highest sensitivity for harbor porpoise hearing, the area over which turbine noise is detectable more than 50% of the time is similar to the effective range for a click detector (100-200 m) (Kyhn et al. 2008; Kyhn et al. 2012). This again suggests a need to stratify analysis by current velocity in order to obtain a high signal to noise ratio for analysis.

This discussion is not intended to discourage studies of turbine noise or marine mammal responsiveness to turbine noise at pilot tidal energy projects, only to provide instructive guidance as to the conditions under which these studies are likely to be most effective. Given the number of assumptions required for this case study, the extent of environmental monitoring will likely require adjustment once post-installation noise characterization is completed (e.g., if turbine noise is higher than predicted at lower

power generation states, detection probabilities would increase). Further, the statistical power to detect behavioral changes will be greater for larger turbine installations or installations in areas with less existing ambient noise than the case study considered here. For example, greater statistical power would be expected for an installation that is detectable to a range of several kilometers in frequency bands audible to marine mammals commonly occurring at a particular site. A better understanding of the acoustic stressor for tidal turbines can, and should, be obtained from pilot scale projects.

4.2 Warning Distance

Results show that the warning distance (i.e., minimum distance to detection of turbine noise) is a strong function of both ambient noise and current velocity for all receiver classes. Because the turbine source level is expected to increase with increasing current velocity, the warning distance also increases with current velocity. This suggests an inherent mitigation measure for the risk of blade strike – as blade rotation rate increases and the consequences of strike become potentially significant, turbine noise is audible at increasingly greater distances. Significantly, warning distance increases as a power of current velocity, meaning that the window of time that a fish or marine mammal can react to turbine noise is greater during periods of strong currents (i.e., more rapid movement during periods of strong currents does not offset the greater warning distance).

5 Conclusions and Recommendations for Future Work

This study presents a pre-installation case study for the extent of tidal turbine noise at a proposed pilot-scale deployment in northern Admiralty Inlet, Puget Sound, Washington. Measurements of a similar turbine at the European Marine Energy Center are presented and a model proposed for extrapolating these measurements to Admiralty Inlet. When taken in the context of pre-installation ambient noise, the noise from turbine operation is not likely to be routinely detected by marine animals at distances greater than a few hundred meters from the project. This suggests that targeted, thoughtful approaches will be required to characterize turbine noise and the responsiveness of marine animals to this noise.

The number of variables involved complicates discussions of turbine noise detection. Variables include spatial positioning of receivers and sources (x,y,z), time-variation in ambient noise, time-variation in turbine noise, and the sensitivity of the receivers at different frequencies. In presenting the results of this assessment, we have, by necessity, chosen to focus on a representative subset of these cases. Much as communicating of this type of probabilistic information is challenging, regulatory agencies involved in the permitting of marine energy projects will be similarly challenged to interpret the biological significance of such information. Developing common frameworks to treat this type of problem is essential.

This case study also highlights a number of high-priority considerations for turbine noise characterization. First, the relation between power generation state and noise produced by turbines should be rigorously established, both with respect to the intensity of noise and frequency of noise. The estimates presented in this study, extending the approach taken by Davidson and Mallows (2005), suggest that understanding this relation could be crucial to developing accurate probabilistic models for the effects of turbine noise. Second, this study has assumed that turbine noise is radiated in an omnidirectional manner. If turbine noise is directional, source level estimates obtained along a single bearing may either under- or over-estimate received levels along other bearings. Third, this study has

only considered detection of noise, not responsiveness of marine animals. For these received levels, Ellison et al. (2012) suggests that a context-based, rather than a dose-response, model is likely to be most effective. Such models require a thorough understanding of received noise levels (intensity, frequency, directionality) and the behavioral state/history of the marine mammal responding to this noise. These, and other, uncertainties are only likely to be reduced through careful monitoring of pilot-scale turbine installations and improved understanding of marine animal responsiveness to noise from various sources.

This case study provides instructive guidance for the range of information needed to plan post-installation monitoring of tidal energy projects. Information needs include the probability distribution of turbine noise (intensity and frequency content), the probability distribution of ambient noise, and any relation between the distribution of turbine noise and distribution of ambient noise.

Acknowledgements

Funding in support of this research is provided by the US Department of Energy and Snohomish Public Utility District. Support for Christopher Bassett is provided by the National Science Foundation under award number DGE-0718124.

Many thanks to Jim Thomson, Capt. Andy Reay-Ellers, Joe Talbert, and Alex DeKlerk for the design and deployment of instrumentation in northern Admiralty Inlet.

Acoustic data from the operating OpenHydro turbine at EMEC were collected by Caroline Carter and Ben Wilson of the Scottish Association for Marine Science.

Marla Holt at the National Oceanic and Atmospheric Administration's Northwest Fisheries Science Center provided a number of helpful comments that motivated this analysis.

References

Ainslie, M.A. and J.G. McColm (1998) A simplified formula for viscous and chemical absorption in sea water, *J. Acoust. Soc. Am.*, 103(3):1671-1672.

Barber, A. (1992) "Handbook of Noise and Vibrational Control", Elsevier Science Publishers, Ltd. Oxford, UK.

Barr, S. (2010) Acoustic characterisation of the Open-Centre turbine. Technical report to Snohomish Public Utility District by OpenHydro.

Basset, C., J. Thomson, and B. Polagye (2010) Characteristics of underwater ambient noise at a proposed tidal energy site in Puget Sound, *MTS/IEEE Oceans 2010*, Seattle, WA September 20-23, 2010.

Bassett, C., B. Polagye, M. Holt, and J. Thomson (submitted) A vessel noise budget for Admiralty Inlet, Puget Sound, WA (USA), submitted to *J. Acoust. Soc. Am.*

Bassett, C., J. Thomson, and B. Polagye (in prep) – Shifting gravel and cobbles as a source of ambient noise.

Carter, C. (2007) Marine renewable energy devices: A collision risk for marine mammals? Masters' thesis, University of Aberdeen, UK.

Cavagnaro, R., B. Polagye, J. Wood, and D. Tollit (in prep) – Assessing trends in harbor porpoise echolocation activity.

Davison, A. and T. Mallows (2005) Strangford Lough Marine Current Turbine environmental statement, Royal Haskoning technical report 9P5161/R/TM/Edin, June 15, 2005.

Denardo, C., M. Dougherty, G. Hastie, R. Leaper, B. Wilson, and P.M. Thompson (2001) A new technique to measure spatial relationships with groups of free-ranging coastal cetaceans, J. Appl. Ecol., 38(4):888-895.

Emery, W.J. and R.E. Thomson (2001) "Data analysis methods in physical oceanography", Elsevier, B.V., Amsterdam, The Netherlands.

Cada, G., J. Ahlgrimm, M. Bahleda, T. Bigford, S. Damiani-Stavrakas, D. Hall, R. Moursund, and M. Sale.(2007) Potential impacts of hydrokinetic and wave energy conversion technologies on aquatic environments, *Fisheries* 32(4):174-181.

Ellison, W.T., B.L. Southall, C.W. Clark, and A.S. Frankel (2011) A new context-based approach to assess marine mammal behavioral responses to anthropogenic sounds. *Cons. Bio.,* 26(1):21-28.

Graber, J., J. Thomson, B. Polagye, and A. Jessup (2011) Land-based infrared imagery for marine mammal detection, *SPIE Photonics+Optics*, San Diego, CA, August 20-25, 2011.

Hatch, L. C. Clark, R. Merrick, S. Van Parijs, D. Ponirakis, K. Schwehr, M. Thompson, and D. Wiley (2008) Characterizing the relative contributions of large vessels to total ocean noise fields: A case study using the Gerry E. Studds Stellwagen Bank National Marine Sanctuary, *Environmental Management,* 42:735-752.

Hazelwood, R. and Connelly, J. (2005) Estimation of underwater noise – a simplified method. *International J. Soc. Underwater Technology*, 26:51-57.

Kastelein, R.A., P. Bunskoek, M. Hagedoorn, W. Au, and D. de Haan (2002) Audiogram of a harbor porpoise (*Phocoena phocoena*) measured with narrow-band frequency-modulated signals, *J. Acoust. Soc. Am.*, 112(1):334-344.

Kastak, D. and R.J. Schusterman (1998) Low-frequency amphibious hearing in pinnipeds: Methods, measurements, noise, and ecology, *J. Acoust. Soc. Am.*, 103(4):2216-2228.

Kyhn, L., J. Tougaard, J. Teilmann, M. Wahlberg, P. Jørgensen, and N. Bech (2008) Harbor porpoise (Phocoena phocoena) static acoustic monitoring: laboratory detection thresholds of T-PODs are reflected in field sensitivity, *J. Mar. Bio. Assoc. UK*, 88:1085-1091, DOI: 10.1017/S0025315408000416

Kyhn, L., J. Tougaard, L. Thomas, L.R. Duve, J. Stenback, M. Amundin, G. Desportes (2012) From echolocation clicks to animal density—Acoustic sampling of harbor porpoises with static dataloggers, *J. Acoust. Soc. Am.*, 131(1), 550-560.

Lee, S., S-R Kim, Y-K Lee, JR Yoon, and P-H Lee (2011) Experiment on effect of screening hydrophone for reduction of flow-induced ambient noise in ocean, *Jap. J. Appl. Phys.*, 50, DOI: 10.1143/JJAP.50.07HG02.

Ma, B., J. Nystuen, and R-C. Lien (2005) Prediction of underwater sound levels from rain and wind, J. Acoust. Soc. Am., 117(6):3555-3565.

Marsh H.W. and M. Schulkin (1962) Shallow water transmission, *J. Acoust. Soc. Am.*, 34:863–864

Madsen, P.T., M. Johnson, P.J.O. Miller, N. Aguilar Soto, J. Lynch, and P. Tyack (2006) Quantitative measures of air-gun pulses recorded on sperm whales (*Physeter macrocephalus*) using acoustic tags during controlled exposure experiments, *J. Acoust. Soc. Am.*, 120(4): 2366-2379.

McKenna, M., D. Ross, S. Wiggins, and J. Hilderbrand (2012) Underwater radiated noise from modern commercial ships, *J. Acoust. Soc. Am.*, 131(1):92-103.

McQuinn, I.H., V. Lesage, D. Carrier G. Larrivee, Y. Samson, S. Chartrand, R. Michaud, and J. Theriault (2011) A threatened beluga (*Delphinapterus leucas*) population in the traffic lane: Vessel-generated noise characteristics of the Sageunay-St. Lawrence Marine Park, Canada, *J. Acoust. Soc. Am.*, 130(6):3661-3673.

Miller, P. (2006) Diversity in sound pressure levels and estimated active space of resident killer whale vocalizations, J. Comp. Phys. A Neuroethology, Sensory, Neural, and Behavioral Physiology, 192(5):449-459.

National Research Council of the U.S. National Academies (NRC) (2003) *Ocean Noise and Marine Mammals*, National Academy Press, Washington, DC.

National Research Council of the U.S. National Academies (NRC) (2005) *Marine Mammal Populations and Ocean Noise: Determining When Ocean Noise Causes Biologically Significant Effects*, National Academy Press, Washington, DC.

Ocean Renewable Power Company (2011) Application of ORPC Maine, LLC for a hydrokinetic pilot project license for the Cobscook Bay Tidal Energy Project, Federal Energy Regulatory Commission Docket P-12711, Sept. 1, 2011.

Polagye, B., B. Van Cleve, A. Copping, and K. Kirkendall, K. (eds.) (2011a) Environmental effects of tidal energy development: Proceedings of a scientific workshop, March 22-25, 2010. NOAA Technical Memorandum NMFS F/SPO-116.

Polagye, B., C. Bassett, and J. Thomson (2011b) Estimated Received Noise Levels for Marine Mammals from OpenHydro Turbines in Admiralty Inlet, Washington et al., Technical report, University of Washington, Seattle, WA.

Polagye, B. and J. Thomson (*submitted*) Tidal energy resource characterization: methodology and field study in Admiralty Inlet, Puget Sound, US. Submitted to *Proc. IMechE, Part A: J. Power and Energy*.
Popper, A.N., and M.C. Hastings (2009) The effects of anthropogenic sources of sound on fishes, *J. Fish. Bio.*, 75(3):455-489.

Richardson, W.J., C.R. Greene, C.I. Malme, and D.H. Thomson (1995) Marine mammals and noise, Academic Press, Elsevier, San Diego, CA, USA.

Snohomish Public Utility District (2009), Draft license application for the Admiralty Inlet tidal project, Federal Energy Regulatory Commission Docket P-12690, Dec. 28, 2009.

Southall, B., Bowles, A., Ellison, W., Finneran, J., Gentry, R., Greene, C., Kastak, D., Ketten, D., Miller, J., Nachtigall, P., Richardson, W., Thomas, J., Tyack, P. (2007) Marine mammal noise exposure criteria: initial scientific recommendations. *Aquatic Mammals*, 33 (4).

Terhune, J.M. (1988) Detection thresholds of a harbor seal to repeated underwater high-frequency short-duration pulses*, Can. J. Zoo.*, 66(7):1578-1582.

Tougaard, J., O.D. Henriksen, and L.A. Miller (2009) Underwater noise from three types of offshore wind turbines: Estimation of impact zones for harbor porpoises and harbor seals, J. Acoust. Soc. Am., 125(6):3766–3773.

Twidell, J. and T. Weir (2006) "Renewable energy resources", Taylor & Francis, New York, NY.

Urick, R. (1983) "Principles of Underwater Sound", McGraw-Hill.

Verdant Power (2010) Final license application for hydrokinetic pilot project license for Roosevelt Island tidal energy project, Federal Energy Regulatory Commission Docket P-12611, Dec. 29, 2010.

Wartzok, D. and D.R. Ketten (1999) Marine mammal sensory systems, in *Biology of Marine Mammals*, J. Reynolds and S. Rommel (eds.), Smithsonian Institution Press, pp. 117-175.

Wartzok, D., A.N. Popper, J. Gordon, and J. Merrill (2003) Factors Affecting the responses of marine mammals to acoustic disturbance. *Marine Technology Society Journal*, *37*(4), 6-15.

Wenz, G. (1962) Acoustic ambient noise in the ocean: Spectra and sources, *J. Acoust. Soc. Am.*, 34:1936-1956.